A Model for Granular Texture with Steric Exclusion

H. Troadec, Farhang Radjai, S. Roux, J. C. Charmet

Model for granular texture with steric exclusion

H. Troadec,[1] F. Radjai,[1] S. Roux,[2] and J. C. Charmet[3]
[1]*LMGC, CNRS–Université Montpellier II, Place Eugène Bataillon, 34095 Montpellier Cedex, France*
[2]*Laboratoire Surface du Verre et Interfaces, CNRS–Saint Gobain, 39 Quai Lucien Lefranc, 93303 Aubervilliers Cedex, France*
[3]*LPMMH, ESPCI, 10 Rue Vauquelin, 75231 Paris Cedex 05, France*

(Received 12 March 2001; revised manuscript received 22 March 2002; published 15 October 2002)

We propose a method to characterize the geometrical texture of a granular packing at the particle scale including the steric hindrance effect. This method is based on the assumption of a maximum directional disorder (statistical entropy) compatible with both the strain-induced anisotropy of the contact network and steric exclusions. We show that the predicted statistics for the local configurations are in fairly good agreement with our numerical data.

DOI: 10.1103/PhysRevE.66.041305 PACS number(s): 81.05.Rm, 05.60.−k

I. INTRODUCTION

Modeling granular media from a microscopic standpoint poses a difficult problem: How does the spatial organization of particles control the behavior at the macroscopic scale? A basic observation is that the flow and failure properties of granular materials arise mainly from the geometrical frustration of particles induced by contact, friction, and excluded-volume effects [1]. For this reason, the rheology is likely to depend on more subtle structural properties than that encountered in other multibody materials or models of disordered media [2].

A very elementary effect of mutual exclusions is that a particle may be simultaneously touched by only a few neighboring particles. The coordination number (the number of touching neighbors) cannot exceed six in a two-dimensional (2D) assembly of particles of nearly the same size and 12 in a 3D packing. These *local environments* fluctuate strongly in space in terms of both coordination numbers and the angular positions of the neighbors.

Another important observation is that the relative angular positions of the particles, i.e., the directions of contact normals, are not isotropically distributed [3,4]. Due to this structural anisotropy, the strength of a granular material is dependent on strain orientation. In the language of plasticity, this means that the texture anisotropy, along with dilatancy, behaves as an internal variable for strain-stress characteristics of the material. This observation shows the central role of the contact network and its directional organization for granular media.

The adequate description of local environments accounting for the geometrical features mentioned above, namely, a combination of excluded-volume constraints, disorder, and anisotropy, is a crucial step in tracing back the rheology of granular materials to the particle scale. Consider, for instance, a granular packing in static equilibrium. The force balance on a particle involves the angular positions of the contact neighbors belonging to the local environment of the particle. The requirement that two neighbors may not occupy angular positions closer than a finite angle $\delta\theta$ (approximately $\pi/3$ for particles of nearly the same size; see Fig. 1) drastically reduces the accessible equilibrium configurations of the contact neighbors and hence those of the whole packing. This effect is obviously enhanced at incipient failure and for large anisotropies. While the texture anisotropy has been considered by several authors as a fundamental structural factor for the behavior of granular materials [3], the key role of steric exclusions has almost always been disregarded in this context.

In this paper, we propose a statistical model of local environments that incorporates steric hindrances, disorder, and structural anisotropy. We apply this model to a two-dimensional packing and we solve the resulting equation. The predicted statistics for local environments will then be compared with raw data from numerical simulations.

II. DESCRIPTION OF GRANULAR TEXTURE

Let us consider the simple model of a 2D packing of rigid disks. In simulations or experiments in 2D geometry, a weak polydispersity is necessary to avoid local crystalline order. In our theoretical description, as we shall see below, the geometrical disorder is explicitly taken into account through the coordination number and the contact directions. We may thus assume that the particles are of the same size, and the steric hindrance will be characterized by a single exclusion angle $\delta\theta = \pi/3$.

A. Global texture

The directional organization of the contact network is described by the probability density function (PDF) of contact

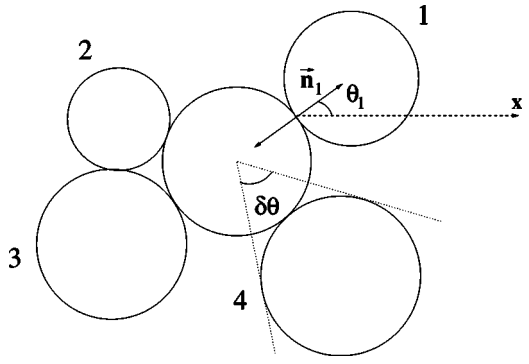

FIG. 1. Schematic representation of a particle environment with $z=4$ contact neighbors. The angle θ_i is the angular position of particle i and $\delta\theta$ is the exclusion angle.

normals $p(\theta)$ [6–9]. This is the probability that a particle has a contact along θ, the polar angle of the contact normal $\vec{n}$; Fig. 1. This distribution is induced by the relative motions of the particles, reflecting thus the deformation history or the dynamics of the preparation process. The function $p(\theta)$ is π periodic (no intrinsic orientation can be attributed to a contact). It is often assumed that $p(\theta)$ can be approximated by its truncated Fourier transform [8]

$$p(\theta)=\frac{1}{\pi}\{1+a\cos 2(\theta-\theta_p)\}, \tag{1}$$

where a represents the texture anisotropy and θ_p is the average contact direction. This functional form is reasonable for a simple deformation history, but it may considerably deviate from this simple form otherwise [7,9,10]. In order to bypass a particular fitting form such as Eq. (1) for characterizing the anisotropy, one may consider instead the ''fabric tensor'' $\boldsymbol{F}\equiv\langle\vec{n}\otimes\vec{n}\rangle$ where the angular brackets denote averaging over all contacts in a representative element of volume, and $\otimes$ is the dyadic product [11,12]. Then, the texture anisotropy a is defined to be $a=2|F_1-F_2|$ where F_1 and F_2 are the eigenvalues of $\boldsymbol{F}$.

A richer description of the texture is provided by the PDF $f_z(\theta)$ that a particle with z contact neighbors has one neighbor at the angular position θ. This function is defined over the range $[0,2\pi]$ and it can be Fourier expanded, as in Eq. (1), but the corresponding anisotropy coefficients now will depend on z. At leading order in θ, we have

$$f_z(\theta)=\frac{1}{2\pi}\{1+a_z\cos 2(\theta-\theta_z)\}. \tag{2}$$

It is important to point out here that the steric exclusions do not allow for arbitrary global distributions f_z. For f_z defined by Eq. (2), the anisotropy a_z could take any values in the range $[0,1]$ ($a_z\geqslant 1$ implies negative values of f_z for some directions, whereas negative values can be avoided by turning θ_z into $\theta_z+\pi/2$). Nevertheless, the steric exclusions impose an upper bound a_{max} on the anisotropy. Indeed, at most one contact can be found within an angular sector of $\pi/3$ around a particle, i.e.,

$$\int_{\theta-\pi/6}^{\theta+\pi/6} z f_z(\theta)\,d\theta\leqslant 1, \tag{3}$$

which together with the expression of f_z given Eq. (2) yields

$$a_{max}(z)=\frac{4\pi}{\sqrt{3}}\left(\frac{1}{z}-\frac{1}{6}\right). \tag{4}$$

This shows that a_{max} decreases with increasing z and becomes zero for $z=6$. In order to evaluate f_z for a granular sample, the subset of particles with z contacts are to be singled out. Our numerical simulations show that a_z, calculted for these subsets, indeed decreases with increasing z [13].

B. Local texture

The above PDF's are, however, insufficient to represent the local environments. A complete description requires the coordination number z of a particle and the angular positions $\theta_1,\ldots,\theta_z$ of its contact neighbors. The particle environments are then characterized by a *multicontact* PDF $g_z(\theta_1,\ldots,\theta_z)$. This is a 2π-periodic function. By definition, the integration of g_z over all angles but one, θ_k, should give back the global distribution $f_z(\theta_k)$ introduced above:

$$\int_{\mathcal{E}_z(k)} g_z(\{\theta_i\})\,d\{\theta_i\}_{i\neq k}=f_z(\theta_k), \tag{5}$$

where $\mathcal{E}_z(k)$ is the domain corresponding to integration from 0 to 2π over all the θ_i except θ_k.

III. THE MODEL

Here, we would like to construct the local PDF's $g_z(\{\theta_i\})$ from the global distribution $f_z(\theta)$. Of course, the solution is not unique since g_z contains much richer information than does f_z. The point, however, is to get a solution that incorporates the required local information with no bias toward a particular solution. In the absence of local steric constraints, the most *unbiased* situation implies

$$g_z(\theta_1,\ldots,\theta_z)=\prod_{i=1}^{z} f_z(\theta_i). \tag{6}$$

In our case, this solution is wrong since the steric exclusions require

$$g_z(\{\theta_i\})=0 \quad \text{if} \quad |\theta_i-\theta_j|<\pi/3, \tag{7}$$

for $i\neq j$. However, this basic requirement is not met by the above solution.

The solution that we propose is still to resort to a similar least biased assumption, provided the above steric constraints are taken into account. This solution allows us to take into account the intrinsic disorder of the granular medium incorporating at the same time the required information (steric constraints and anisotropy). But it is clear that this approximation cannot be verified otherwise than by comparing the resulting solutions with suitable experiments or numerical simulations.

Operationally, this solution translates into the maximization of an entropy functional $S[g_z]$ under constraints. According to Shannon's entropy, we have

$$S[g_z]=-\int_{\mathcal{D}_z} g_z(\{\theta_i\})\ln[g_z(\{\theta_i\})]\,d\{\theta_i\}, \tag{8}$$

where $\mathcal{D}_z=([0,2\pi])^z$ is the integration domain. This functional should be maximized over the set of functions that satisfy both the steric exclusions Eq. (7) and the normalization conditions Eq. (5). We note that the entropy formalism, as a basic statistical tool, has been previously applied to

granular materials in order to characterize other aspects of a random packing such as the coordination number and the void ratio [14].

Equation (7) implies that the maximization of S should be restricted to a domain $\mathcal{A}_z$ (inside $\mathcal{D}_z$) allowed by steric exclusions. Indeed, the maximization applies only to the lacking information, and here the value of g_z is already known ($g_z=0$) for the angles belonging to the excluded region $\mathcal{B}_z=\mathcal{D}_z-\mathcal{A}_z$. Thus, this restriction accounts for the steric constraints. The normalization conditions [Eq. (5)] can be imposed through Lagrange multipliers. This leads to the maximization of the functional

$$T[g_z]=S[g_z]-\sum_{i=1}^{z}\int_0^{2\pi}\lambda_i(\theta_i)C_i[g_z]d\theta_i \tag{9}$$

over $\mathcal{A}_z$, where the $\lambda_i(\theta_i)$ are the Lagrange multipliers and

$$C_i[g_z]=f_z(\theta_i)-\int_{\mathcal{E}_z(i)}g_z(\{\theta_i\})d\{\theta_k\}_{k\neq i}. \tag{10}$$

The solution of the above equation can be determined by setting the functional derivative of $T[g_z]$ to zero. Let us remark that here the only correlations among the angles are the steric exclusions themselves. This means that the angles θ_i can be considered as independent variables when they are restricted to the allowed domain A_z. As a consequence, the solution is given by a product of identical functions h of a single angle in the allowed domain. Thus, the general solution takes the following form:

$$g_z(\{\theta_i\})=\left(\prod_{i\neq j}G(\theta_i-\theta_j)\right)\prod_{k=1}^{z}h_z(\theta_k), \tag{11}$$

where $G(\theta)$ is a 2π-periodic function such that $G(\theta)=0$ for $|\theta|<\pi/3$, and $G=1$ otherwise. These prefactors take care of the steric exclusions. Note that, in the absence of steric exclusions, we would have $G=1$ for all angles and the solution (6) would be recovered with $h_z(\theta)\equiv f_z(\theta)$.

The function h_z is fixed by the normalization condition (5). In terms of h, this condition takes the form of the following implicit equation:

$$\int_{\mathcal{A}_z(i)}\prod_{k=1}^{z}h_z(\theta_k)d\{\theta_j\}_{j\neq i}=f_z(\theta_i), \tag{12}$$

where $\mathcal{A}_z(i)=\mathcal{E}_z(i)\cap\mathcal{A}_z$. This equation can be used for a numerical computation of h_z for a given f_z.

We used an iterative scheme over the functions $u_n(\theta)$ satisfying

$$u_{n+1}(\theta_1)=\epsilon u_n+(1-\epsilon)\frac{f_z(\theta_1)}{\int_{A_z(1)}u_n(\theta_2)\cdots u_n(\theta_z)d\theta_2\cdots d\theta_z}, \tag{13}$$

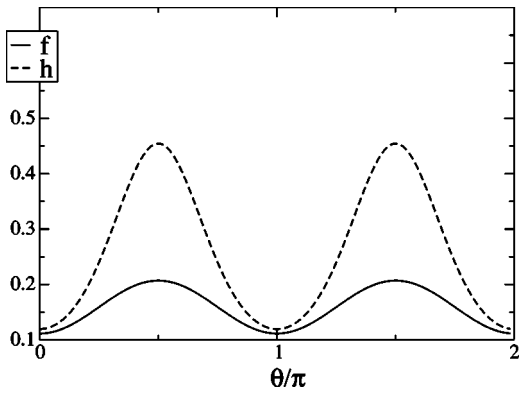

FIG. 2. The function $h_3(\theta)$ calculated for $f_3(\theta)$ with $a_3=0.3$ by solving Eq. (13).

where ϵ is a relaxation parameter. The solution h_z of Eq. (12) is simply a fixed point of the latter recursion. This iterative process converges quite smoothly to the solution when the latter exists and its convergence domain matches exactly the set of admissible values of the anisotropy given by Eq. (4). One example is shown in Fig. 2: The function $h_3(\theta)$ was computed according to the above procedure with $f_3(\theta)$ given by Eq. (2) for $z=3$ and $a_3=0.3$. We see that h_3 has the same monotony as f_3, but it deviates from a simple sinusoidal form.

IV. COMPARISON WITH SIMULATIONS

Of course, it is desirable to compare the multicontact distributions g_z predicted by the above approach with direct data from experimental or numerical observations. However, a sufficient statistical precision requires very large samples. In fact, given a granular sample, the subset of particles with z contacts should be considered. Assuming that in a 2D system of disks the number of particles is the same for each of the prevailing values 3, 4, and 5 of z, then only nearly one-

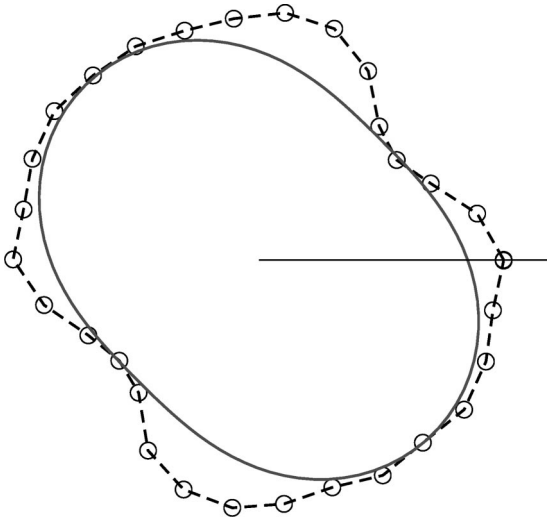

FIG. 3. Distribution $f_4(\theta)$, represented in polar coordinates, evaluated for a simulated sample under simple shear (circles) and fitted by a simple sinusoidal form (solid curve).

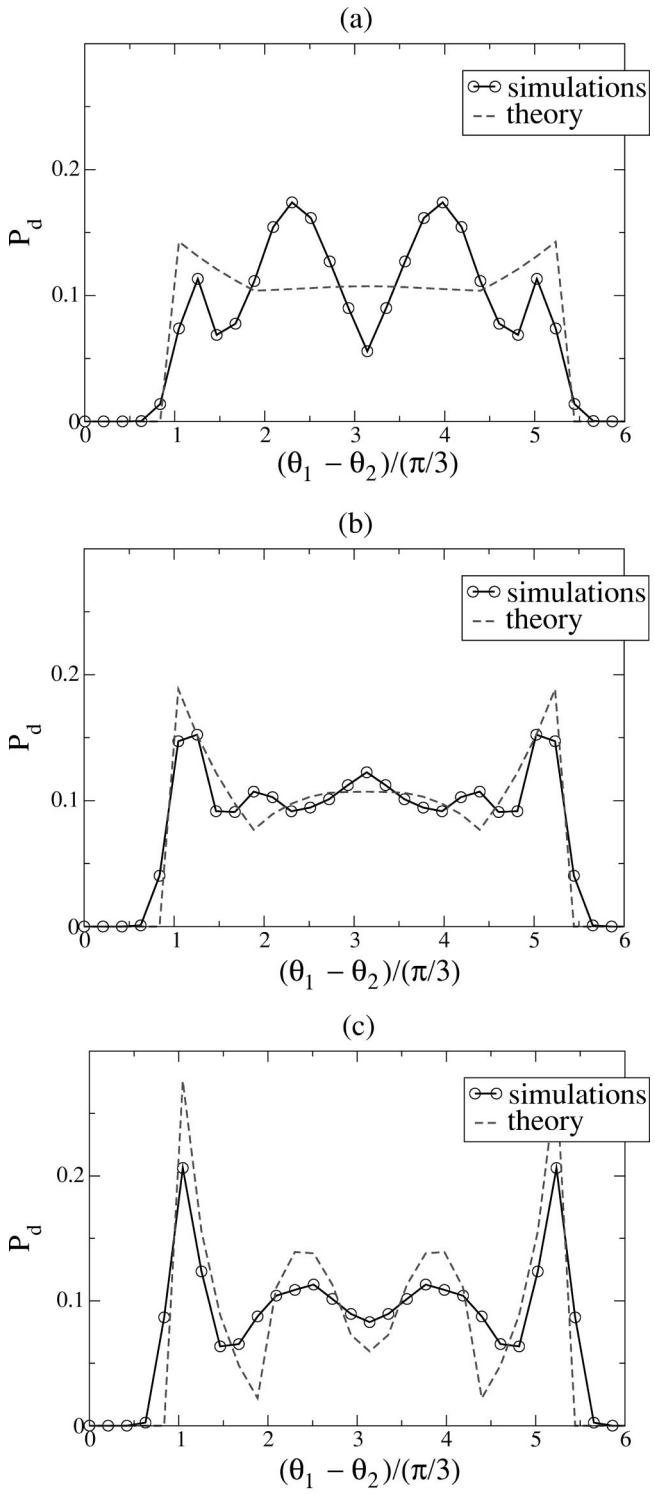

FIG. 4. Probability density function $p(\Delta\theta)$ of the difference $\Delta\theta$ between the angular positions of contact neighbors of a particle with $z=3$ (a), $z=4$ (b), and $z=5$ (c), as predicted by our model and evaluated by means of numerical simulations.

third of particles will be available for the evaluation of g_z. On the other hand, subdividing the interval $[0,2\pi]$ into n angular sectors and requiring on average m events in each elementary box in $[0,2\pi]^z$, one needs a sample of $m(n^z)$ contacts, or approximately $(2m/z)n^z$ particles. For $z=4$, $n=20$, and $m=100$, this amounts to 8×10^6 particles. This is inaccessible in practice with present-time computation power.

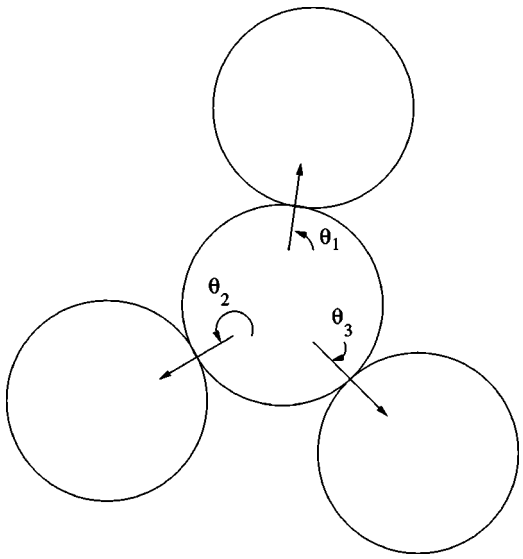

FIG. 5. Representation of a typical particle environment with $z=3$ contact neighbors. The force balance requirement here is as important as the steric hindrances.

Nevertheless, we still may get a reliable comparison by focusing on the distributions $p_d(\Delta\theta)$ of the difference $\Delta\theta=|\theta_1-\theta_2|$ between contact directions extracted from pair distributions $p_2(\theta_1,\theta_2)$. The latter was calculated from both numerical samples and the theoretical estimation of g_z. To do this, we performed numerical simulations of a system of 4000 particles with biperiodic boundary conditions by means of the molecular dynamics method. We used a viscous-regularized Coulomb friction law and a linear spring-dashpot model for particle interactions [5]. The coefficient of friction was 0.5 and the particle radii were uniformly distributed between R_1 and R_2 with $R_2=2R_1$. The system was subjected to simple shearing and because of the biperiodic boundary conditions we were able to keep shearing in the steady state for very large strains without wall effects. The global steady-state anisotropy a calculated from the fabric tensor was about 0.13.

The global PDF's f_z obtained from these simulations will be used below as input to the model for comparison with simulations. For the sake of illustration, in Fig. 3 we have shown $f_4(\theta)$ in polar coordinates corresponding to the subset of particles in the numerical sample with four contact neighbors. We see that a simple fitting form such as Eq. (2) may be used as a reasonable approximation as long as the anisotropy a_4 is is the relevant information for the texture. For comparison with the model, we preferred, however, to use the numerical PDF's f_z as input to the model for the calculation of g_z in order to avoid discrepancies arising from the input data. We emphasize that our main concern in this paper is not the shape of the global PDF's f_z or p, but the relation between these global distributions and the local multicontact PDF's g_z.

The distribution p_d was calculated over accumulated data from several well-separated snapshots of the steady state for the set of particles with coordination number z. For the theoretical evaluation of $p_d, f_z(\theta)$ as input for the calculation of g_z following our model was used. Then, the distributions p_2 and p_d were extracted from g_z.

In Fig. 4 we have plotted the theoretical and numerical p_d as a function of $\Delta\theta$ for $z=3$, $z=4$, and $z=6$. Although only the geometrical constraints are taken into account for the theoretical construction of g_z (no force considerations), we see that the predicted distributions p_d for both $z=4$ and $z=5$ fit the numerical data fairly well . The fit is better for $z=5$ than for $z=4$. On the other hand, the fit for $z=3$ is much less satisfactory. The numerical curves show additional peaks around $2\pi/3$ and $4\pi/3$ for $z=3$. These peaks clearly correspond to configurations such as the one shown in Fig. 5. Such configurations happen frequently since they satisfy best the force balance for a particle with only three contact neighbors, whereas the model incorporates only steric constraints at the particle scale in addition to the global texture anisotropy. In fact, in going from $z=3$ to $z=5$, the requirement of force balance becomes less and less stringent, while steric exclusions increasingly dominate the behavior.

V. CONCLUDING REMARKS

Our results suggest that, even if only the steric exclusions are taken into account at the particle scale, a satisfactory evaluation of the statistics of local environments in terms of the functions g_z can be obtained at least for $z=4$ and $z=5$. The steric exclusions control to a large extent the local distributions (Fig. 4) and reduce the range of admissible anisotropies [Eq. (4)].

A natural extension of our model, at the cost of additional parameters, is to include force balance as well as steric exclusions at the particle scale. Then, both contact directions and contact forces should be considered in the model. The forces are coupled to a local stress tensor in the same way as the contact directions were coupled to the fabric tensor. The entropy of local distributions is then maximized taking into account constraints arising from steric exclusions and the force balance requirement, as well as contact laws such as the positivity of normal forces and Coulomb's law of friction.

Apart from its importance in itself as a general model for granular texture including steric exclusions, the characterization of the texture in terms of local environments is a crucial step in order to relate the macroscopic behavior to the particle scale. For example, the range of admissible stresses can be studied by considering representative configurations generated according to the multicontact statistics of local environments [13]. A similar procedure based on entropy formalism may be applied as well to other relevant microscopic configurations, such as cells composed of contiguous particles that carry local strains.

[1] H.M. Jaeger and S.R. Nagel, Rev. Mod. Phys. **68**, 1259 (1996).
[2] J. M. Ziman, *Models of Disorder* (Cambridge University Press, Cambridge, England, 1979).
[3] *Behavior of Granular Media*, edited by B. Cambou (Springer, Vienna, 1998); *Mechanics of Granular Materials*, edited by M. Oda and K. Iwashita (Balkema, Rotterdam, 1999).
[4] S. Roux and F. Radjai, in *Physics of Dry Granular Media*, edited by H. Herrmann, J.-P. Hovi, and S. Luding (Kluwer, Dordrecht, 1997), pp. 229–236.
[5] S. Luding, in *Physics of Dry Granular Media* [4], pp. 285–304.
[6] M. Oda and J. Koshini, Soils Found. **14**, 25 (1974).
[7] B. Cambou, in *Powders and Grain 93*, edited by C. Thornton (Balkema, Rotterdam, 1993), pp. 73–86.
[8] R.J. Bathurst and L. Rothenburg, Mech. Mater. **9**, 65 (1990).
[9] F. Calvetti, G. Combe, and J. Lanier, Mech. Cohesive-Frict. Mater. **2**, 121 (1997).
[10] F. Radjai and S. Roux, in *Powders and Grain 2001* (Balkema, Lisse, 2001), pp. 21–24.
[11] M. Satake, Theor Appl. Mech. **26**, 257 (1978).
[12] J. Goddard, in *Physics of Dry Granular Media* (Ref [4]), pp. 1–24.
[13] H. Troadec *et al.* (unpublished).
[14] B. F. Backman *et al.*, in *Advances in the Mechanics and the Flow of Granular Materials*, edited by M. Shahinpoor (Trans Tech Publications, Clausthal-Zellerfeld, 1983), Vol. 1, pp. 259–272.